TRENDS IN SCIENCES 2026; 23(9): 13022
https://doi.org/10.48048/tis.2026.13022 RESEARCH ARTICLE

Passage Culture to Assemble A *Ganoderma*-Suppressive Microbiome from Turmeric (*Curcuma Longa*) Root Exudates

Latifa Karunia[1], Suwandi Suwandi[1,2,*], Ahmad Muslim[2], Rahmat Pratama[2] and Rahmad Fadli[2]

[1]*Plant Sciences Graduate Program, Faculty of Agriculture, Universitas Sriwijaya, South Sumatra 30662, Indonesia*
[2]*Department of Plant Protection, Faculty of Agriculture, Universitas Sriwijaya, South Sumatra 30662, Indonesia*

([*]Corresponding author's e-mail: suwandi@fp.unsri.ac.id)

Received: 14 December 2025, Revised: 25 January 2026, Accepted: 1 February 2026, Published: 5 April 2026

Abstract

Ganoderma boninense, the causative agent of basal stem rot (BSR), poses a significant threat to global oil palm cultivation. Turmeric (*Curcuma longa*) rhizome is recognized as a potential source of a suppressive microbiome for biocontrol applications. This study aimed to investigate the efficacy of passage culture in assembling a highly suppressive microbiome from turmeric root exudates against *G. boninense*. The initial microbiome, collected as turmeric root exudate (T0), was used to inoculate sucrose medium, which was then supplemented with fresh turmeric rhizome (T), chitin powder (C), T plus *G. boninense* culture (TG), or TG plus chitin (TGC). This inoculation process constituted the 1st passage, and the culture was continuously passaged up to 10 or 20 times by transferring the harvested culture filtrate into fresh medium. The results revealed that bacteria isolated from the 5th passage cultures of both the TG5 and TGC5 treatments exhibited the strongest antagonism, causing 46% and 45% inhibition of *Ganoderma* colony growth, respectively. *Ganoderma* mycelia treated with these bacteria experienced thinning and lysis of the cell wall. Furthermore, treatment with the passage bacteria induced *Ganoderma* cell leakage, as indicated by the increased electrical conductivity (EC) values of the inhibitory *Ganoderma* colonies. 16S rRNA gene amplicon sequencing identified *Gluconacetobacter sacchari*, *Nguyenibacter vanlangensis*, and *Novosphingobium humi* as the dominant species in the TG5 and TGC5 passage cultures. In conclusion, pathogen-driven assembly of a suppressive microbiome via *in vitro* passage culture offers a promising host-independent strategy for *G. boninense* biocontrol.

Keywords: Passage culture, *Ganoderma boninense*, Turmeric root exudates, Suppressive microbiome, Antagonistic bacteria

Introduction

Basal Stem Rot (BSR), caused by the fungal pathogen *Ganoderma boninense*, constitutes the most significant biological threat to the oil palm (*Elaeis guineensis*) industry, particularly throughout Southeast Asia [1]. Since its recognition in the 1960s, BSR has inflicted substantial economic losses, with yield reductions ranging from 50% to 80% reported in severely affected plantations [2]. The distinct BSR symptoms, including leaf yellowing, unopened young fronds, and the presence of *G. boninense* fruiting bodies at the stem base, reflect extensive damage to the palm's vascular system, leading to restricted water uptake and, ultimately, plant mortality [1,3]. Of particular concern is the pathogen's rapid spread in replanting areas and converted lands, resulting in high infection rates even in newly established plantations [4]. Furthermore, the high adaptability of *G. boninense* to various soil types, including both mineral and peat soils [5,6], and its ability to infect oil palm at all growth stages significantly complicates current management strategies [3].

Biological control strategies utilizing allelopathic companion plants offer a promising, sustainable approach against chronic diseases like BSR. Previous studies have demonstrated that intercropping oil palm with perennial herbs, such as taro [7], ginger (*Zingiber officinale*), and Java turmeric (*Curcuma xanthorrhiza*), can significantly inhibit *G. boninense* infections and reduce pathogen inoculum potential [8]. The suppressive effect observed in oil palms intercropped with these rhizomatous herbs is primarily attributed to their root exudates. Root exudates are complex mixtures of organic compounds released into the rhizosphere, including carbohydrates, organic acids, amino acids, and specialized secondary metabolites [9]. These exudates act as both a food source and signaling molecules, fundamentally shaping the associated microbial community by stimulating the recruitment of beneficial soil microorganisms. This interaction is critical for plant health, as the recruited microbes enhance nutrient uptake, disease resistance, and overall plant growth [10].

Root exudates represent a critical interface between plants and their surrounding microbiomes, often exerting direct antifungal effects through the release of bioactive compounds. For instance, wheat root exudates contain phytosphingosine, which not only inhibits *Fusarium oxysporum* f. sp. *niveum* but also modulates the watermelon rhizosphere microbiome to suppress pathogen invasion [11]. Similarly, isoliquiritigenin and lauric acid have been identified as potent antifungal metabolites effective against *Phytophthora nicotianae*, the causal agent of tobacco black shank disease [12]. More recently, Karlina *et al*. [13] demonstrated that microbial-origin biocompounds, including azelaic acid, bis(2-ethylhexyl) phthalate, haplofungin, and piptamine, are highly expressed in inhibitory root exudates against *G. boninense*. Collectively, these findings underscore the potential of root exudate-microbe interactions as eco-friendly biocontrol agents.

Although the pivotal role of root exudates in shaping rhizosphere microbiomes is well established [14], the direct utilization and *in vitro* assembly of microbial communities specifically harbored within root exudates for disease suppression remains largely unexplored. Suppressive soils and pathogen-suppressive microbiomes have long been recognized as reservoirs of antagonistic microbes, often assembled through successive monoculture planting [15]. Likewise, phyllosphere microbial communities can be experimentally passaged between environments to generate foliar disease-suppressive consortia [16]. Passage, in this context, entails the successive transfer and cultivation of microbial consortia from one host to another, thereby enriching functional traits and adaptive capacities. We developed a host-independent framework to assemble a *Ganoderma*-suppressive microbiome using *in vitro* passage culture. This approach utilizes pathogen-driven selection to enrich specialized microbial communities derived from turmeric root exudates.

Materials and methods

Culture setup and enrichment medium

Liquid cultures were established in glass jars equipped with two-port caps, serving as an air inlet for aeration and an outlet for gas exchange. Each culture vessel contained 200 mL of a 2% sucrose solution supplemented with specific enrichment materials. The enrichment treatments consisted of: (1) 25 g of fresh whole turmeric rhizome (T); (2) half a plate of a 7-day-old *G. boninense* culture (G) grown on Malt Extract Agar (MEA); and (3) 1.25 g of chitin powder (C) (30 - 60 mesh, degree of deacetylation > 84%). Turmeric rhizomes were sourced from a local market. The study was conducted in two sequential trials, with three batches each. Trial 1 evaluated three enrichment treatments: T, C, and GC (G+C). Trial 2 evaluated two enrichment treatments: TG (T+G) and TGC (T+G+C).

Passage culture procedure

Passage culture was performed to progressively select for a *Ganoderma*-suppressive microbiome from the initial turmeric root exudate community. The initial microbiome (T0) was collected from root exudates of turmeric plants grown in cocopeat medium fertilized with compost extract [13]. The passage procedure was carried out for up to 20 passages in Trial 1 and 10 passages in Trial 2. The first passage (1st passage) was initiated by inoculating 200 mL of the enrichment medium (containing sucrose and the designated treatment materials) with 50 mL of the T0 microbiome. The culture was fermented with continuous aeration for two days at room temperature (25 - 28 °C). For

subsequent passages, 150 mL of the liquid culture was harvested and filtered through a 100-mesh nylon filter; the filtrate is hereafter referred to as the culture filtrate. A 50 mL aliquot of this culture filtrate was then used as the inoculant for the next passage containing fresh medium. The remaining culture filtrate was stored at 4 °C for further analysis.

Assessment of antifungal activity

The antifungal activity of the bacterial communities from the passage cultures was assayed *in vitro* using the paper disc method [17]. Culture filtrates were harvested at T0 (initial microbiome) and at passages 5, 10, 15, and 20 for Trial 1, and at passages 1, 5, and 10 for Trial 2. Bacterial cell suspensions derived from these harvested culture filtrates were used as the treatments. These suspensions were prepared by harvesting 1 mL of the culture filtrate, followed by centrifugation at 12,000 rpm for 10 min. The supernatant was discarded, and the bacterial pellet was washed twice with sterile 10 mM $MgCl_2$ to remove residual medium [18]. The washing process involved resuspension, vortexing, and centrifugation under the same conditions. Finally, the washed bacterial pellet was resuspended in 0.5 mL of sterile 10 mM $MgCl_2$. Sterile filter paper discs were impregnated with 20 µL of the final bacterial suspension and placed on MEA plates inoculated with *G. boninense*. Six Petri plates were used as replicates for each treatment. Inhibitory activities were evaluated based on three parameters: Colony growth inhibition, microscopic morphological changes, and the electrical conductivity (EC) of the medium.

Colony growth inhibition assay

The percentage of inhibition was determined by comparing the colony area of *G. boninense* treated with filter paper discs containing the bacterial suspension against the untreated control colonies. Colony area was measured on the fifth day post-treatment using ImageJ software (version 1.54k, National Institutes of Health). The percentage of *G. boninense* mycelial growth inhibition (I) was calculated using the following formula [19].

$$I = \frac{(C-T)}{C} \times 100\% \quad (1)$$

where C is the colony area of *Ganoderma* in the control plate and T is the colony area in the treatment plate.

Microscopic morphological analysis

For morphological analysis, a segment of the *Ganoderma* colony edge adjacent to the inhibition zone was excised and mounted on a glass slide. The slides were incubated in moist chambers (Petri dishes lined with wet tissue paper) for three days to allow hyphal growth. Following incubation, the agar blocks were carefully trimmed to expose the mycelium growing on the slide surface. The mycelium was stained with lactophenol cotton blue, covered with a coverslip, and examined under a compound microscope to observe cellular abnormalities.

Evaluation of electrical conductivity (EC)

The impact of bacterial treatments on *G. boninense* membrane permeability was assessed by measuring the electrical conductivity (EC) of the culture medium [20]. On day 5 of the assay, *Ganoderma* colonies from the treated plates were excised into four equal sections and immersed in 10 mL of distilled water for one hour. The EC value of the immersion water was subsequently measured using a LAQUAtwin EC-22 meter (HORIBA Advanced Techno, Co., Ltd., Japan). Increased EC values indicate electrolyte leakage due to membrane disruption.

Metagenomic analysis

To characterize the bacterial community composition, a 1-mL aliquot from the passage cultures was harvested for DNA extraction. Total genomic DNA was extracted using the ZymoBIOMICS DNA Miniprep Kit (Zymo Research, Irvine, CA, USA) according to the manufacturer's instructions. A total of 30 ng of high-quality DNA was used as the template for PCR amplification of the 16S rRNA gene. PCR products were purified using AMPure XP magnetic beads and subsequently used for library construction. Library size and concentration were validated using the Agilent 2100 Bioanalyzer (Agilent Technologies, USA). Sequencing was performed on a DNB-based sequencing platform (MGI Tech Co., Ltd., China) following standard protocols.

Bioinformatic processing involved raw read quality filtering and adapter removal using using fastp

v0.23.4 [21], followed by read merging and chimera removal using VSEARCH v2.22.1 [22]. High-quality sequences were processed in QIIME2 v2024.10, where amplicon sequence variants (ASVs) were inferred using the DADA2 algorithm [23]. Taxonomic assignment was performed against the SILVA v138.2 reference database [24].

Statistical analysis, including Partial Least Squares Discriminant Analysis (PLS-DA), was performed to visualize community differences and identify discriminant taxa [25]. ASVs with a Variable Importance in Projection (VIP) score > 2.0 and relative abundance > 1% were classified as dominant discriminant taxa [26]. Differential abundance among treatments was analyzed using the DESeq2 package (v1.50.2) in R [27,28]. Raw count data were modeled using negative binomial generalized linear models, and significance was evaluated using the Wald test [28]. *p*-values were adjusted for multiple comparisons using false discovery rate (FDR) control approaches and ASVs with an adjusted *p*-value < 0.05 were considered significantly differentially abundant [27].

Results and discussion

Inhibitory effects of Passage-cultured bacteria on *ganoderma*

In the first trial, passage cultures were conducted up to the 20th passage using sucrose medium enriched with either turmeric (T) or chitin (C). Bacterial communities isolated from the 5th to the 20th passage cultures (T-5 to T-20 and C-5 to C-20) exhibited weak antagonistic activity against *Ganoderma boninense*. The inhibition rates were relatively low, ranging from 19.5% to 30.5% for the T-series and 21.0% to 33.3% for the C-series. Visually, the *Ganoderma* colonies displayed an irregular growth front with localized clear zones immediately surrounding each bacterial-impregnated disc (**Figure 1**). Statistical analysis revealed no significant differences ($p > 0.05$) in inhibition rates across the different passage cycles. Although inhibition peaked slightly at the 5th, 10th, and 15th passages, it declined by the 20th passage (**Figure 1**). Notably, chitin enrichment tended to yield communities with marginally higher inhibitory activity compared to turmeric alone. Furthermore, the electrical conductivity (EC) values of the medium treated with these bacterial communities did not differ significantly ($p > 0.05$) across the passage cycles (**Figure 2**).

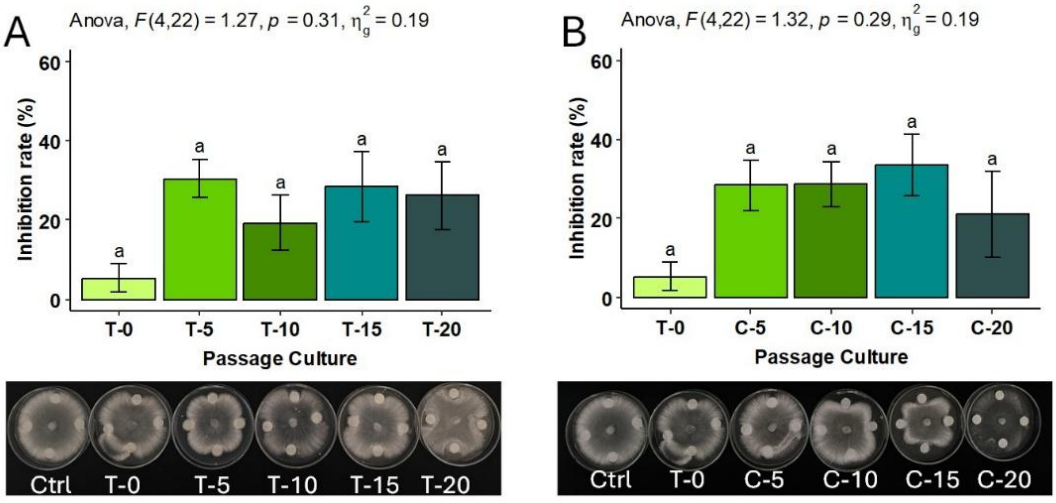

Figure 1 Inhibition rate and visual inhibitory effects of bacteria-impregnated filter paper discs on *Ganoderma boninense*. Bacteria were derived from serial passage cultures (passages 0, 5, 10, 15, and 20) in medium enriched with turmeric rhizome (T) (A, D) or chitin (C) (B, C). Error bars represent the standard error of the mean (SEM) derived from three trial batches, with six Petri plates used as replicates per treatment. Bars labeled with the same letter are not significantly different according to Tukey's HSD test ($p < 0.05$).

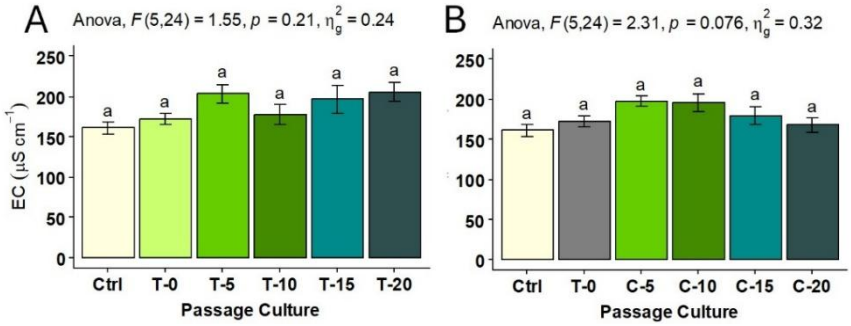

Figure 2 Electrical conductivity (EC) values of MEA medium colonized by *Ganoderma boninense* and treated with serially cultured bacteria (passages 0, 5, 10, 15, and 20). Bacterial communities were enriched in medium supplemented with turmeric rhizome (T) (A) or chitin (C) (B). Error bars represent the standard error of the mean (SEM) derived from three trial batches, with six Petri plates used as replicates per treatment. Bars labeled with the same letter are not significantly different according to Tukey's HSD test ($p < 0.05$).

In the second trial, passage culture was conducted using sucrose medium supplemented with turmeric rhizome plus *Ganoderma* culture (TG) or turmeric rhizome plus *Ganoderma* culture plus chitin (TGC). In contrast to the first trial, bacterial consortia derived from the passage cultures were associated with significant inhibition of *Ganoderma* colony growth. The *Ganoderma* colonies displayed distinct irregular growth fronts with prominent zones of suppressed mycelial development (**Figure 3**). While the initial microbiome (T0) showed only marginal inhibition (8.1%), serial passage in both TG and TGC media appeared to effectively enrich the antagonistic potential. Notably, the TGC medium demonstrated a high level of inhibition as early as the 1st passage, which remained consistent through the 5th passage. In contrast, the TG treatment appeared to reach its peak suppressive activity at the 5th passage (TG5, 46%), achieving an inhibition level comparable to that observed in the TGC5 passage (45%) (**Figure 3**). However, this suppressive activity appeared to decrease by the 10th passage in both treatments.

Paper disc assays utilizing the suppressive bacterial communities significantly ($p < 0.05$) increased the EC values of the *Ganoderma*-colonized medium (**Figure 4**). This elevation in EC was consistently observed in all inhibitory treatments, with the most pronounced effects recorded in the 5th and 10th passage cultures (**Figure 4**). The significantly increased EC values suggest an association between the presence of the bacterial community and potential membrane permeability disruption, likely contributing to electrolyte leakage in *G. boninense* hyphae.

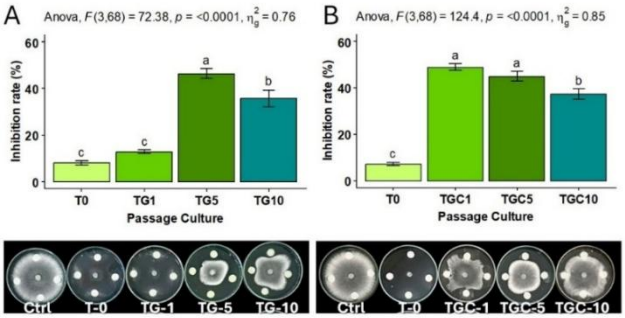

Figure 3 Inhibition rate and inhibitory effects on *Ganoderma boninense* colony growth by bacteria serially cultured (passages 0, 1, 5, and 10) in sucrose medium enriched with turmeric rhizome + *G. boninense* (TG) (A) or turmeric rhizome + *G. boninense* + chitin (TGC) (B). Error bars represent the standard error of the mean (SEM) derived from three trial batches, with six Petri plates used as replicates per treatment. Bars labeled with the same letter are not significantly different according to Tukey's HSD test ($p < 0.05$).

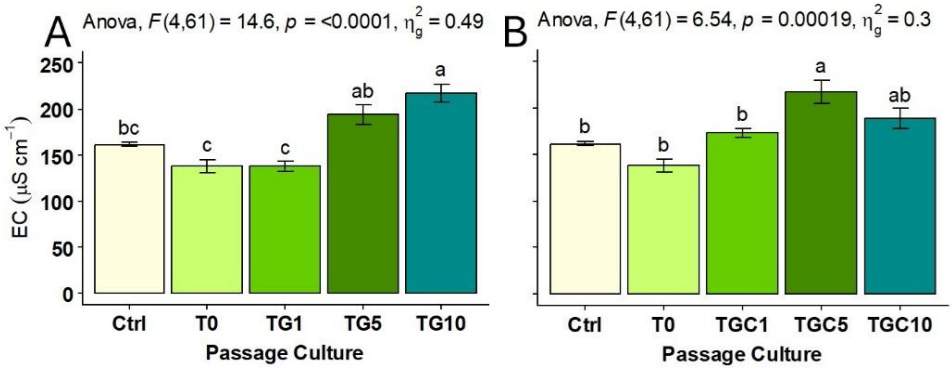

Figure 4 Electrical conductivity (EC) values of MEA medium colonized by *Ganoderma boninense* and treated with bacteria serially cultured (passages 0, 1, 5, and 10). Enrichment media were sucrose supplemented with turmeric rhizome + *G. boninense* (TG) (A) or turmeric rhizome + *G. boninense* + chitin (TGC) (B). Error bars represent the standard error of the mean (SEM) derived from three trial batches, with six Petri plates used as replicates per treatment. Bars labeled with the same letter are not significantly different according to Tukey's HSD test ($p < 0.05$).

Treatment with bacteria derived from the TG and TGC passage cultures induced severe morphological alterations in *G. boninense*. The treated mycelium exhibited progressive thinning of the cell wall, which eventually led to hyphal collapse. In control samples, the cell walls stained intensely blue with lactophenol cotton blue, indicating intact chitin structures. In contrast, this staining was markedly reduced or completely absent in hyphae treated with the passage bacteria, providing evidence of possible damage to the outer cell wall and septal regions. Microscopic observations indicated hyphal deterioration, which appeared to be characterized by disruption and potential lysis of the cell wall structure (**Figure 5**).

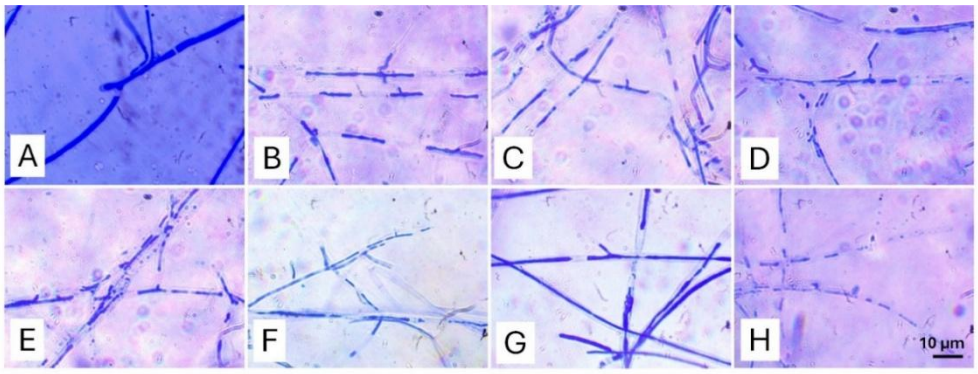

Figure 5 Microscopic morphology of *Ganoderma boninense* mycelium at the inhibition zone edge. Treatments: (A) Control (10 mM $MgCl_2$); (E) Initial turmeric root exudate bacteria (T0); (B) - (D) Bacteria from passages 1, 5, and 10 in TG medium (turmeric + *Ganoderma*); (F) - (H) Bacteria from passages 1, 5, and 10 in TGC medium (turmeric + *Ganoderma* + chitin).

This study successfully demonstrates that passage liquid culture, an approach previously utilized for evolving microbial communities in the phyllosphere [16], can be effectively adapted *in vitro* to assemble a specialized *Ganoderma*-suppressive microbiome from turmeric root exudates. The results from Trial 1 (T and C enrichments) show that sequential passage alone, even with simple nutrient enrichment, yields only weak antagonism (19.5% to 33.3% inhibition), and the suppressive capability tends to decline by the 20th passage. This decline suggests that continuous passage on a basic sucrose medium lacks the necessary selective pressure to stably enrich functional antagonistic communities.

In contrast, the inclusion of both the fresh turmeric rhizome (as a complex organic substrate) and the target

pathogen (*G. boninense*) in the medium (TG and TGC) appeared to be a key factor influencing functional assembly. This combined approach enhanced the antagonistic activity dramatically, reaching maximum inhibition (45% - 46%) at the 5th passage. This phenomenon highlights that effective *in vitro* microbiome assembly requires an "ecological driving force", where the presence of the pathogen acts as a selective filter, forcing the microbial community to evolve or enrich members capable of competitive exclusion or direct biocontrol [15]. The decline observed at the 10th passage, despite the initial enhancement, suggests that the optimal selective pressure or resource availability window is narrow, occurring specifically around the 5th transfer cycle.

Metagenomic analysis of passaged culture

The dynamics of bacterial composition were evaluated using 16S rRNA gene amplicon sequencing, comparing the initial turmeric root exudate microbiome (T0) with the 5th passage cultures (TG5 and TGC5). The combined dataset comprised 478 Amplicon Sequence Variants (ASVs). Partial Least Squares Discriminant Analysis (PLS-DA) revealed distinct clustering of T0, TG5, and TGC5 communities, indicating significant shifts in microbiome composition following the passage process (**Figure 6(A)**). Alpha diversity analysis showed a sharp decline in species richness. The ACE (Abundance-based Coverage Estimator) value for TG5 (17.7) was significantly lower than that of the initial T0 community (105.3), confirming a strong selective bottleneck. The ACE value for TGC5 was 72.7, which did not differ significantly from the other groups.

A total of 26 species belonging to 16 genera were observed to be dominant (relative abundance > 1%) across the treatments (**Figure 6(B)**). Of these, 12 taxa had a PLS-DA Variable Importance in Projection (VIP) score > 2.0, suggesting their potential roleas key discriminant species. The initial root exudate fermentation (T0) was dominated by *Gluconacetobacter asukensis* (relative abundance 42.6%), *Sporolactobacillus spathodeae* (21.5%), *Paraburkholderia tropica* (7.7%), and *Tumebacillus flagellatus* (1.9%). The 5th passage culture supplemented with turmeric rhizome and *Ganoderma* mycelium (TG5) resulted in a major shift in bacterial composition, dominated by: *Gluconacetobacter sacchari* (30.8%), *Nguyenibacter vanlangensis* (30.5%), *G. asukensis* (14.9%), *Paraburkholderia tropica* (7.7%), *Novosphingobium humi* (7.6%), and *Beijerinckia mobilis* (5.4%). Notably, *N. vanlangensis* and *N. humi* were not detected in the initial T0 microbiome. The 5th passage passage culture supplemented with turmeric rhizome, *Ganoderma* mycelium, and chitin powder (TGC5) yielded a more diverse set of dominant species, including: *Sporolactobacillus kofuensis* (28.2%), *G. sacchari* (18.1%), *N. humi* (15.0%), *Azotobacter tropicalis* (5.7%), *Leuconostoc mesenteroides* (3.3%), and an uncultured *Novosphingobium* sp. (1.0%). Species that showed significantly higher abundance in both TG5 and TGC5 compared to T0 included *G. sacchari* and *N. humi*. Additionally, *A.tropicalis*, *L. mesenteroides*, and the uncultured *Novosphingobium* sp. showed significantly higher abundance in the TGC5 treatment (**Figure 7**).

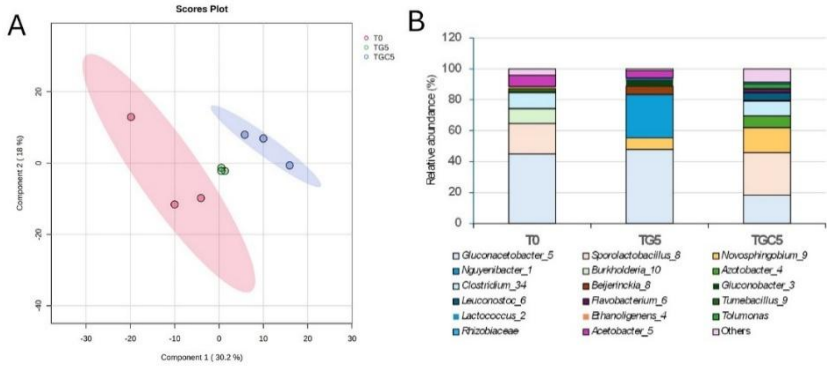

Figure 6 (A) PLS-DA score plot and (B) relative abundance of bacterial genera in the initial turmeric root exudate (T0) compared 5th passage cultures enriched with turmeric rhizome + *Ganoderma boninense* (TG5) or turmeric rhizome + *G. boninense* + chitin (TGC5). The number following each genus name indicates the count of identified species.

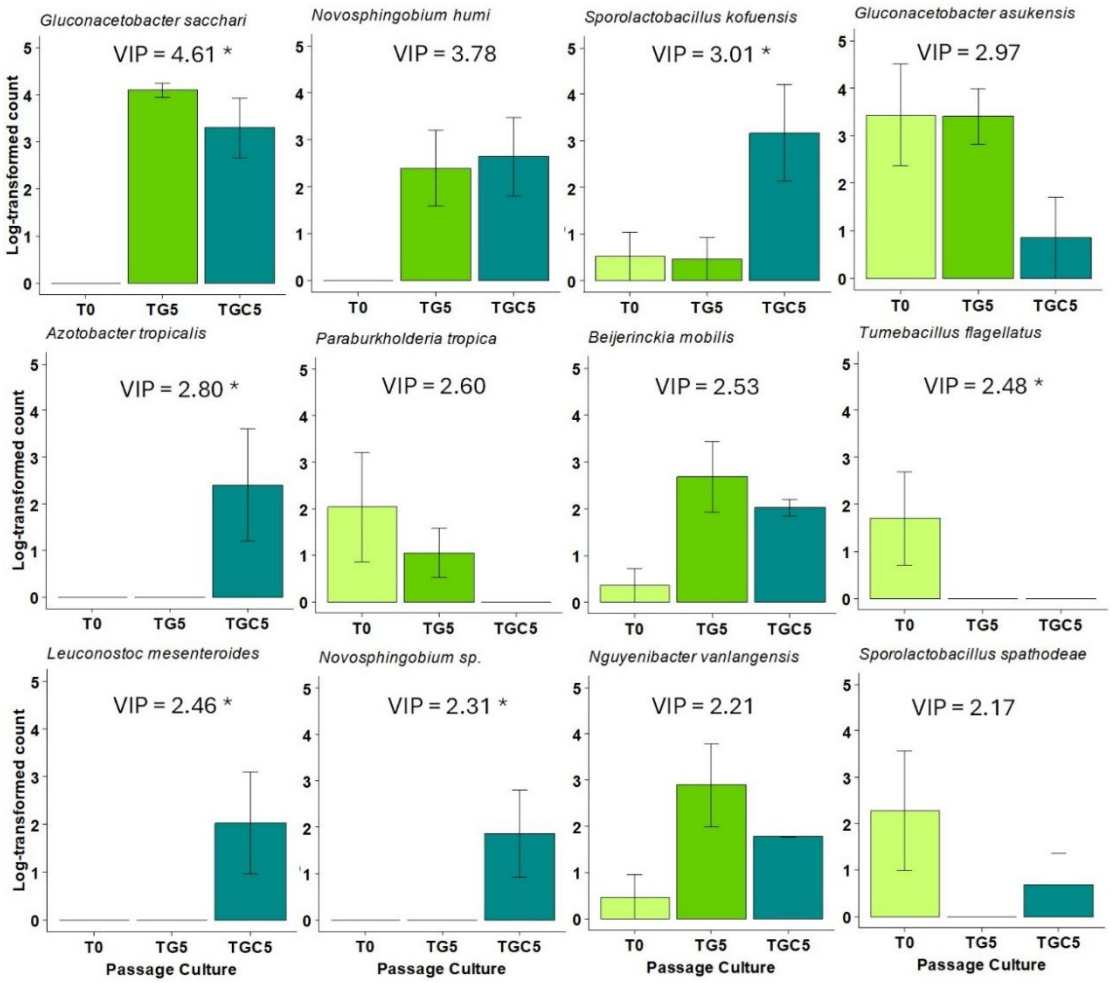

Figure 7 Differential abundance of dominant and highly discriminant species (PLS-DA VIP score > 2) comparing the initial microbiome (T0) with the 5th passage cultures: Turmeric + *Ganoderma boninense* (TG5) and turmeric + *G. boninense* + chitin (TGC5). Asterisks (*) denote statistically significant differences in abundance based on the Wald test (FDR-adjusted $p < 0.05$).

The 16S rRNA sequencing data provide an indication of how the passage culture may have shifted the microbiome from an exudate-dominated community (T0) toward a community associated with pathogen suppression (TG5/TGC5). The clear separation of the T0, TG5, and TGC5 groups in the PLS-DA score plot, along with the sharp decline in alpha diversity (ACE from 105.3 in T0 to 17.7 in TG5), confirms that the enrichment and passage process acted as a strong selective bottleneck, successfully reducing overall species richness while enriching specific functional taxa [29]. The initial T0 community was dominated by typical root-associated taxa, notably *G. asukensis* and *S. spathodeae*. However, the 5th passage was characterized by a shift toward taxa often associated with antagonistic or beneficial functions. The most significant shift observed in the metagenomic analysis was the strong selection for *G. sacchari* and the emergence of *N. vanlangensis* and *N. humi*, neither of which was detected in the initial T0 community.

Gluconacetobacter sacchari dominated both the TG5 and TGC5 communities. This genus typically produces organic acids, such as acetic acid, which may inhibit fungal growth by acidifying the local environment [30]. The strong enrichment of both *N. vanlangensis* and *N. humi* in the suppressive passaged culture suggests they play a critical role in the enhanced antagonism. *Nguyenibacter vanlangensis* is known as an acetic acid bacterium belonging to the α-*Proteobacteria* and has been previously reported as a dominant bacterial endophyte in sugarcane roots. Notably, this species possesses significant plant growth-promoting traits, including the ability to solubilize phosphate, produce siderophores, IAA, and auxin, and it is also able to

inhibit the fungal pathogen *Fusarium moniliforme* [31]. Furthermore, *Novosphingobium* species are widely recognized for their metabolic versatility and production of sphingolipids, which can have potent antimicrobial properties [32]. Supporting this, three sphingolipids, including N-(2-hydroxyhexacosanoyl)-D-sphingosine, N-Tetradecanoyl-4-hydroxy-D-sphingosine, and Isoheptadecasphinganine, were found in the turmeric root exudate samples [13]. These compounds were possibly produced by the *Novosphingobium* species and possess antifungal properties.

The enrichment of specific taxa, such as *G. sacchari*, *N. vanlangensis*, and *N. humi*, under the dual pressure of *G. boninense* and the turmeric substrate, provides a strong associative link to the observed antagonistic effects. While their high relative abundance suggests a potential role in the primary inhibition mechanism, further functional validation via pure-isolate antagonism assays is required to definitively attribute the observed cell lysis to these specific species. Microscopic analysis revealed significant hyphal damage and cell wall collapse in TG5 and TGC5, supporting the observed antagonistic effects. The marked reduction in lactophenol blue staining, which typically binds to chitin [33], points to severe structural compromise. Given that these dominant taxa are not typically primary chitinase producers, an alternative lytic pathway is suspected. This physical degradation was corroborated by a significant increase in electrical conductivity (EC), indicating the leakage of intracellular electrolytes and severe membrane disruption. The concurrence of structural damage and increased EC suggests a mechanism potentially driven by lipophilic metabolites, such as sphingolipids from *Novosphingobium* or organic acids from *Gluconacetobacter*. However, direct isolation and metabolomic profiling are needed to confirm these metabolites as primary drivers of the observed cell wall collapse [34].

Conclusions

This study establishes a novel, host-independent methodology for the *in vitro* assembly of a *Ganoderma*-suppressive microbiome, representing a conceptual shift from traditional rhizosphere studies by utilizing pathogen-driven selection. The bacterial communities isolated from the 5th passage of both TG5 and TGC5 treatments exhibited the strongest antagonism, causing 46% and 45% inhibition of *Ganoderma* colony growth, respectively. Mechanistically, *Ganoderma* mycelia treated with these bacteria underwent severe structural changes, including cell wall thinning and lysis. This damage was further corroborated by increased electrical conductivity (EC) values, confirming significant cell leakage and membrane disruption. Metagenomic analysis identified *G. sacchari*, *N. vanlangensis*, and *N. humi* as the dominant species enriched in the suppressive cultures. Collectively, assembling a suppressive microbiome through passage culture, specifically with the addition of turmeric rhizome and the target pathogen, presents a promising strategy for developing effective biocontrol agents against *G. boninense*.

Acknowledgements

This work was financially supported by a Regular Fundamental Research Grant (109/C3/DT.05.00/PL/2025 and 0042.053/UN9/SB3.LP2M.PT/2025) from the Directorate for Research and Community Service, Ministry of Culture, Research and Technology, the Republic of Indonesia.

Declaration of Generative AI in Scientific Writing

Generative AI tools, namely Google Gemini Plus, were employed exclusively for grammar correction and refinement of language expression. The conception of the study, literature synthesis, data analysis, interpretation of findings, and all aspects of critical discussion were entirely conducted by the author without reliance on AI.

CRediT Author Statement

Latifa Karunia: Investigation, Formal analysis, Visualization, Writing - Original draft preparation, Writing - Review & Editing. **Suwandi Suwandi:** Conceptualization, Methodology, Formal analysis, Resources, Writing - Review & Editing. **Ahmad Muslim:** Supervision, Funding acquisition. **Rahmat Pratama:** Data Curation; Supervision; Funding acquisition. **Rahmad Fadli:** Software; Validation. **Siti Herlinda:** Resources; Validation; Supervision.

References

[1] L Zakaria. Basal stem rot of oil palm: The pathogen, disease incidence, and control methods. *Plant Disease* 2023; **107(3)**, 603-615.

[2] A Kamu, CK Phin, IA Seman, D Gabda and HC Mun. Estimating the yield loss of oil palm due to *Ganoderma* basal stem rot disease by using Bayesian model averaging. *Journal of Oil Palm Research* 2021; **33(1)**, 46-55.

[3] YW Khoo and KP Chong. *Ganoderma boninense*: General characteristics of pathogenicity and methods of control. *Frontiers in Plant Science* 2023; **14**, 1156869.

[4] H Priwiratama, AE Prasetyo and A Susanto. Incidence of basal stem rot disease of oil palm in converted planting areas and control treatments. *IOP Conference Series: Earth and Environmental Science* 2020; **468**, 012036.

[5] MS Ibrahim, IA Seman, MH Rusli, MA Izzuddin, N Kamarudin, K Hasyim and ZA Manaf. Surveillance of *Ganoderma* disease in oil palm planted by participants of the smallholders replanting incentive scheme in Malaysia. *Journal of Oil Palm Research* 2020; **32(2)**, 237-244.

[6] I Virdiana, BP Forster and L Zakaria. Basal stem rot of oil palm: Disease development in mineral and peat soils. *IOP Conference Series: Earth and Environmental Science* 2024; **1308**, 012025.

[7] S Suwandi, M Alesia, RP Munandar, R Fadli, S Suparman, C Irsan and A Muslim. The suppression of *Ganoderma boninense* on oil palm under mixed planting with taro plants. *Biodiversitas* 2024; **25(3)**, 1143-1150.

[8] S Suwandi, RP Munandar, S Suparman, C Irsan and A Muslim. Mixed planting with rhizomatous plants interferes with *Ganoderma* disease in oil palm. *Journal of Oil Palm Research* 2023; **35(2)**, 354-364.

[9] J Sun, J Yang, S Zhao, Q Yu, L Weng and C Xiao. Root exudates influence rhizosphere fungi and thereby synergistically regulate *Panax ginseng* yield and quality. *Frontiers in Microbiology* 2023; **14**, 1194224.

[10] M Gu, J Jin, P Lu, S Yu, H Su, H Shang, Z Yang, J Zhang, P Cao and J Tao. Regulation of root-associated microbiomes and root exudates by different tobacco species. *Chemical and Biological Technologies in Agriculture* 2024; **11**, 151.

[11] C Li, Q Tian, MK Rahman and F Wu. Effect of anti-fungal compound phytosphingosine in wheat root exudates on the rhizosphere soil microbial community of watermelon. *Plant and Soil* 2020; **456**, 223-240.

[12] S Peng, F Shu, Y Lu, D Fan, D Zheng and G Yuan. Quasi-targeted metabolomics revealed isoliquiritigenin and lauric acid associated with resistance to tobacco black shank. *Plant Signaling and Behavior* 2024; **19(1)**, 2332019.

[13] L Karlina, S Suwandi, R Fadli, A Muslim, H Hamidson and C Irsan. Metabolomic profiling and antifungal potential of turmeric (*Curcuma longa*) root exudates against *Ganoderma boninense*. *Biodiversitas* 2025; **26(7)**, 3600-3609.

[14] CX Yang, SJ Chen, XY Hong, LZ Wang, HM Wu, YY Tang, YY Gao and GF Hao. Plant exudates-driven microbiome recruitment and assembly facilitates plant health management. *FEMS Microbiology Reviews* 2025; **49**, fuaf008.

[15] D Schlatter, L Kinkel, L Thomashow, D Weller and T Paulitz. Disease suppressive soils: New insights from the soil microbiome. *Phytopathology* 2017; **107(11)**, 1284-1297.

[16] H Ehau-Taumaunu and KL Hockett. Passaging phyllosphere microbial communities develop suppression towards bacterial speck disease in tomato. *Phytobiomes Journal* 2023; **7(2)**, 233-243.

[17] P Lovecká, G Kroneislová, Z Novotná, J Röderová and K Demnerová. Plant growth-promoting endophytic bacteria isolated from *Miscanthus giganteus* and their antifungal activity. *Microorganisms* 2023; **11**, 2710.

[18] KR Arendt, KL Hockett, SJ Araldi-Brondolo, DA Baltrus and AE Arnold. Isolation of endohyphal bacteria from foliar ascomycota and *in vitro* establishment of their symbiotic associations. *Applied and Environmental Microbiology* 2016; **82(10)**, 2943-2949.

[19] H Ashraf, T Anjum, IS Ahmad, R Ahmed, ZH Aftab and H Rizwana. Phytofabricated silver nanoparticles unlock new potential in tomato plants by combating wilt infection and enhancing plant growth. *Scientific Reports* 2025; **15**, 10527.

[20] YS Chan and KP Chong. Bioactive compounds of *Ganoderma boninense* inhibited methicillin-resistant *Staphylococcus aureus* growth by affecting their cell membrane permeability and integrity. *Molecules* 2022; **27**, 838.

[21] S Chen, Y Zhou, Y Chen and J Gu. Fastp: An ultra-fast all-in-one FASTQ preprocessor. *Bioinformatics* 2018; **34**, i884-i890.

[22] T Rognes, T Flouri, B Nichols, C Quince and F Mahé. VSEARCH: A versatile open source tool for metagenomics. *PeerJ* 2016; **4**, e2584.

[23] BJ Callahan, PJ McMurdie, MJ Rosen, AW Han, AJA Johnson and SP Holmes. DADA2: High-resolution sample inference from Illumina amplicon data. *Nature Methods* 2016; **13**, 581-583.

[24] SC Park and S Won. Evaluation of 16S rRNA databases for taxonomic assignments using a mock community. *Genomics and Informatics* 2018; **16**, e24.

[25] Y Wang and KAL Cao. PLSDA-batch: A multivariate framework to correct for batch effects in microbiome data. *Briefings in Bioinformatics* 2023; **24(2)**, bbac622.

[26] Y Jin, Z Chen, JF White, K Malik and C Li. Interactions between Epichloë endophyte and the plant microbiome impact nitrogen responses in host *Achnatherum inebrians* plants. *Microbiology Spectrum* 2024; **12(4)**, e02574-23.

[27] J Pelto, K Auranen, JV Kujala and L Lahti. Elementary methods provide more replicable results in microbial differential abundance analysis. *Briefings in Bioinformatics* 2025; **26(2)**, bbaf130.

[28] F Abegaz, D Abedini, F White, A Guerrieri, A Zancarini, L Dong, JA Westerhuis, FV Eeuwijk, H Bouwmeester and AK Smilde. A strategy for differential abundance analysis of sparse microbiome data with group-wise structured zeros. *bioRxiv* 2023. https://doi.org/10.1101/2023.07.24.549296

[29] JA Kimbrel, TJ Samo, C Ward, D Nilson, MP Thelen, A Siccardi, P Zimba, TW Lane and X Mayali. Host selection and stochastic effects influence bacterial community assembly on the microalgal phycosphere. *Algal Research* 2019; **40**, 101489.

[30] MR Gloria, JS Oscar, MM Sandra, FG Narmer and T Gonzalo. Evaluation of plant-growth promoting properties of *Gluconacetobacter diazotrophicus* and *Gluconacetobacter sacchari* isolated from sugarcane and tomato in West Central region of Colombia. *African Journal of Biotechnology* 2017; **16(30)**, 1619-1629.

[31] N Pitiwittayakul, D Wongsorn and S Tanasupawat. Characterisation of plant growth-promoting endophytic bacteria from sugarcane and their antagonistic activity against *Fusarium moniliforme*. *Tropical Life Sciences Research* 2021; **32(3)**, 97-118.

[32] A Belmok, FMD Almeida, RT Rocha, CS Vizzotto, MR Tótola, MHS Ramada, RH Krüger, CM Kyaw and GJ Pappas. Genomic and physiological characterization of *Novosphingobium terrae* sp. nov., an alphaproteobacterium isolated from Cerrado soil containing a mega-sized chromid. *Brazilian Journal of Microbiology* 2023; **54(1)**, 239-258.

[33] S Raja, P Subhashini and T Thangaradjou. Differential methods of localisation of fungal endophytes in the seagrasses. *Mycology* 2016; **7(3)**, 112-123.

[34] T Wen, Z Ding, LS Thomashow, L Hale, S Yang, P Xie, X Liu, H Wang, Q Shen and J Yuan. Deciphering the mechanism of fungal pathogen-induced disease-suppressive soil. *New Phytologist* 2023; **238(6)**, 2634-2650.